

Available online at www.sciencedirect.com

Medical Engineering & Physics xxx (2006) xxx–xxx

**Medical
Engineering
& Physics**

www.elsevier.com/locate/medengphy

Development of a synthetic phantom for the selection of optimal scanning parameters in CAD–CT colonography

Tarik A. Chowdhury^{a,*}, Paul F. Whelan^a, Ovidiu Ghita^a, Nicolas Sezille^a, Shane Foley^b

^a *Vision Systems Group, Dublin City University, Dublin 9, Ireland*

^b *Department of Radiology, Mater Misericordiae Hospital, Dublin 7, Ireland*

Received 17 August 2005; received in revised form 13 September 2006; accepted 19 September 2006

Abstract

The aim of this paper is to present the development of a synthetic phantom that can be used for the selection of optimal scanning parameters in *computed tomography* (CT) colonography. In this paper we attempt to evaluate the influence of the main scanning parameters including slice thickness, reconstruction interval, field of view, table speed and radiation dose on the overall performance of a *computer aided detection* (CAD)–CTC system. From these parameters the radiation dose received a special attention, as the major problem associated with CTC is the patient exposure to significant levels of ionising radiation. To examine the influence of the scanning parameters we performed 51 CT scans where the spread of scanning parameters was divided into seven different protocols. A large number of experimental tests were performed and the results analysed. The results show that automatic polyp detection is feasible even in cases when the CAD–CTC system was applied to low dose CT data acquired with the following protocol: 13 mAs/rotation with collimation of 1.5 mm × 16 mm, slice thickness of 3.0 mm, reconstruction interval of 1.5 mm, table speed of 30 mm per rotation. The CT phantom data acquired using this protocol was analysed by an automated CAD–CTC system and the experimental results indicate that our system identified all clinically significant polyps (i.e. larger than 5 mm).

© 2006 IPEM. Published by Elsevier Ltd. All rights reserved.

Keywords: CT colonography; Synthetic phantom; Radiation dose; Polyp detection

1. Introduction

Colon cancer is the second leading cause of cancer deaths in the developed nations [1–3] and numerous studies indicated that early detection and removal of colon polyps is the most effective way to reduce colorectal cancer (CRC) mortality [4–7]. Colonoscopy is widely considered the standard diagnostic technique for the detection of colonic neoplasia [8,9] but it is important to mention that colonoscopy is a highly invasive and time consuming medical investigation [10]. Virtual colonoscopy (VC) or CT colonography (CTC) [11–14] is a minimally invasive medical procedure that has been proposed as an alternative to conventional colonography. Since its introduction by Vining et al. [11] in 1994,

CTC has received extensive attention from research community and many publications have emerged in areas of 3D surface rendering and visualization [15–17], centerline calculation [18], colon unfolding [19] and automated polyp detection [20–34]. Recent publications [22,23,35] indicate that the results returned by the automatic CAD–CTC polyp detection systems in the vast majority of cases closely match or even outperform the human reader performance. It is worth mentioning that the performance of the CAD–CTC systems is constantly improving and this is driven not only by the development of new more sophisticated algorithms for polyp detection but also by the advances in the development of the CT scanners. From this aspect, the current range of the multi-detector CT (MDCT) scanners offers excellent image quality and the typical acquisition period is reduced to 20–30 s for a full abdominal scan.

The major concern associated with CTC is the fact that the patients are subjected to high levels of ionising radia-

* Corresponding author. Tel.: +353 17007636; fax: +353 17005508.
E-mail address: tarik@eeng.dcu.ie (T.A. Chowdhury).

tion. The medical literature indicates that the level of ionising radiation received by the patients during the CT examination varies from 5 to 20 mSv [36–41] and this radiation level may induce cancer in 0.05% of the patients older than 50 years that were subjected to a CT abdominal examination [42]. Cohen [43] indicates in his paper that the risk of inducing cancer in patients is significantly lowered when they are subjected to low-level radiation exposure and an important number of studies were carried out in order to identify the minimal level of radiation dose that can be used in CTC but without a negative impact on the detection of colorectal polyps [41,44–46]. The identification of the optimal scanning parameters (collimation, slice thickness, table speed, reconstruction interval) is a difficult problem and this procedure is applied on synthetic phantoms that are designed to accurately model the human body [47–58]. In this sense, Beaulieu et al. [47] used spherical plastic beads to model polyps while Dachman et al. [48] created false polyps in a pig colon by puckering the mucosa of the colon. Their studies focused on finding the imaging effect of collimation, tube current (pitch) and orientation when they analysed different sizes and types of polyps. Similar studies were performed by Taylor et al. [49] and Springer et al. [50]. Using a different approach, Whithing et al. [51] constructed an air filled acrylic cylinder where polyps of different sizes were attached on the inner side of the acrylic tube and they applied the developed phantom to evaluate the artefacts generated by the collimation and the tube current. Laghi et al. [54] and Embleton et al. [55] used synthetic and pig colons and their tests indicate that CT scans with a collimation of $4\text{ mm} \times 2.5\text{ mm}$, 1.25 mm reconstruction interval, 40 mAs/rotation generate datasets with sufficient resolution to be used for automated and manual CTC polyp detection. Ozgun et al. [56] used latex material to build phantom polyps having dimensions ranging from 1 to 10 mm. Their tests were focused on finding the minimal tube current that allows the detection of polyps larger than 5 mm. They reported that the detection of the polyps larger than 5 mm is feasible only if the CT scans are performed in the range 60–100 mAs/rotation.

In this paper we evaluate the effect of key scanning parameters (mAs/rotation, slice thickness, reconstruction interval, field of view and table speed) by analysing the CT data obtained by scanning a novel synthetic phantom. The phantom has been specifically designed for CAD–CTC to simulate colon polyps with different shapes (pedunculated, sessile and flat) and sizes (3–18 mm). In our studies the CT phantom data is evaluated using an automated CAD–CTC system [34] in order to determine the influence of the scanning parameters on polyp detection. A special emphasis of our study is placed on determining the minimal radiation dose that allows robust identification of colonic polyps but not at the expense of reduced sensitivity in polyp detection. This paper is organized as follows. In Section 2 the development of the synthetic phantom is detailed. Section 3 briefly presents the automated CAD–CTC polyp detection system. In Section 4 the experimental results are presented and discussed while Section 5 concludes this paper.

2. Materials and methods

2.1. Phantom design

A synthetic phantom was constructed using a PVC tube, two acrylic tubes, two plastic plates and latex material to emulate the colon wall, polyps and folds. The external PVC tube is 230 mm long with a diameter of 300 mm. Acrylic tubes are 235 mm long and the dimensions of the inner and outer diameters are 40 and 50 mm, respectively. *Hounsfield unit* (HU) values of the PVC tube, acrylic tubes and plastic plates are 1500, 100, 90, respectively. The construction of the synthetic phantom is illustrated in Fig. 1.

The polyp inserts for phantom were made using latex material having a HU value of -95 . We have chosen to use latex as this material allows us to generate very realistic shapes (pedunculated, sessile, flat, flat-depressed) for polyps and folds as illustrated in Fig. 2. In addition the HU values associated with the latex material approximate the HU

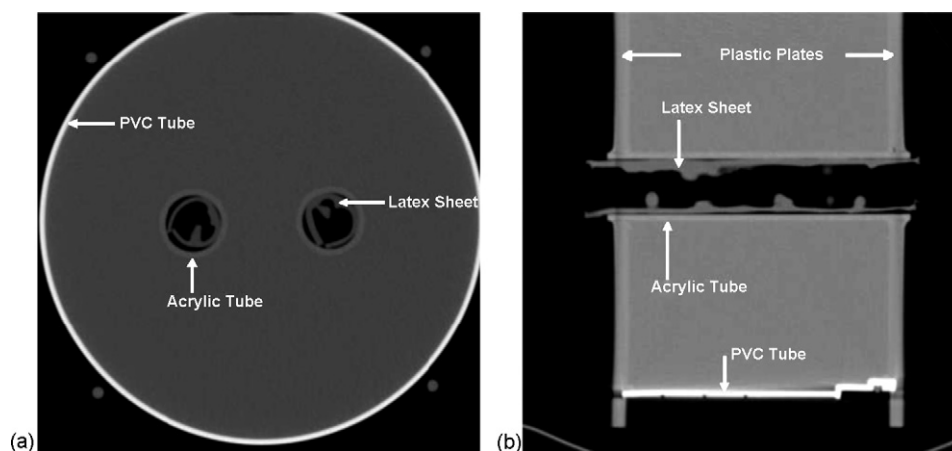


Fig. 1. Synthetic colon phantom: (a) longitudinal view; (b) transversal view.

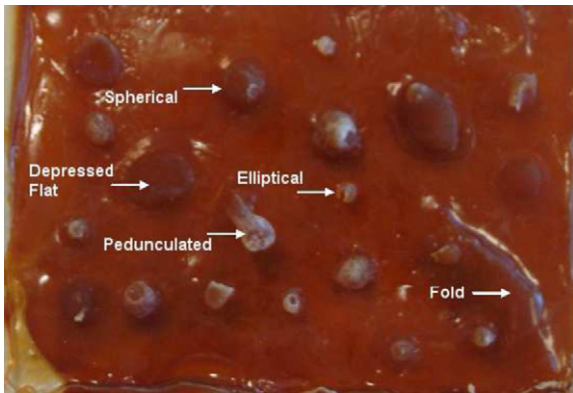


Fig. 2. Latex insert sheet with various types of polyps and folds.

values of the colon wall (~10 HU). In CTC the large difference between the HU values associated with the air voxels (-1000 HU) and the HU values of the colon tissue are evaluated to identify the surface of the colon wall. The model for polyps was made from clay and liquid latex was poured into the model to create the latex polyp inserts. To make the surface of the latex sheet more realistic the thickness of the sheet was made uneven. We have created two sheets of latex containing 48 polyps having different sizes, seven flat

polyps, two depressed flat polyps, 15 non-spherical polyps, two pedunculated polyps, 22 spherical/elliptical polyps and six haustral folds. In Fig. 3 several 3D views of some representative synthetic polyps are depicted.

2.2. Image acquisition

The developed phantom described in Section 2.1 was scanned using a 16-slice Siemens Somatom Sensation CT scanner in Mater Hospital, Dublin, Ireland. The phantom has been scanned in longitudinal (phantom was placed parallel to the CT scanner bed) and transversal directions, where the scanning parameters (collimation, slice thickness, field of view, table speed, reconstruction interval and mAs/rotation) were varied. All scans were performed at 120 kVp tube voltage. It is useful to note that the effective radiation dose is influenced by the value of the tube voltage but its relationship with image quality, tissue contrast and image noise is complex and the effect of this parameter would be difficult to be evaluated. Therefore, in our experiments we maintained the value of this parameter constant (120 kVp) because this is the standard value of the tube voltage used in most clinical examinations. The smoothing reconstruction filter used was the B30 filter [59] and this filter has been employed based on

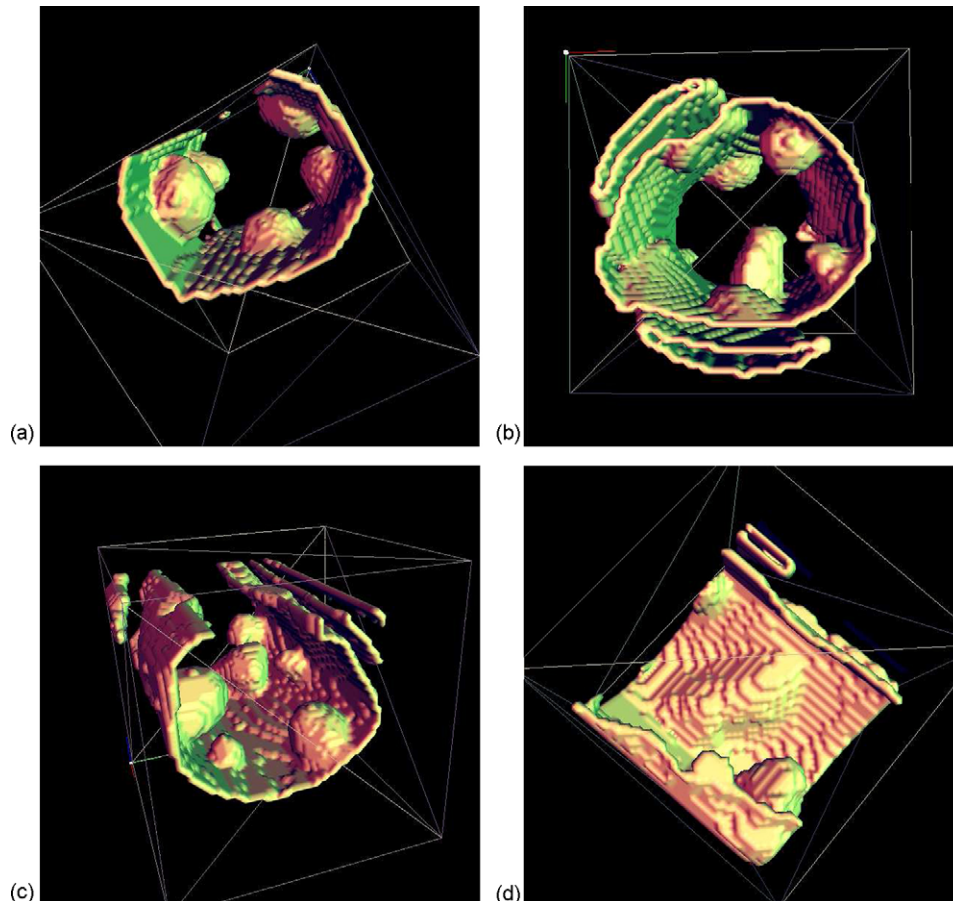


Fig. 3. Three-dimensional longitudinal views of the synthetic polyps (a–c) and fold (d) made from latex.

its optimal performance in data smoothing and noise removal (this is the filter used in most clinical studies and a detailed evaluation on the performance of the available smoothing filters is beyond the scope of this investigation).

In conjunction with our clinical partners from Mater Hospital we have chosen the following spread of parameters: collimation $0.75\text{ mm} \times 16\text{ mm}$ and $1.5\text{ mm} \times 16\text{ mm}$, field of view: 325 and 360 mm, table speed: 20–30 mm/rotation, slice thickness of 1, 2 and 3 mm and mAs/rotation: 100, 80, 70, 60, 50, 40, 30, 20 and 13 (13 mAs/rotation is the minimum value that can be set for Siemens Somatom Sensation CT scanner used in our experiments). These scanning parameters have been divided into seven protocols as follows:

- Protocol 1: Collimation $1.5\text{ mm} \times 16\text{ mm}$, slice thickness 3 mm, reconstruction interval 1.5 mm, field of view 325 mm, table speed 30 mm/rotation, mAs/rotation: 100, 80, 70, 60, 50, 40, 30, 20 and 13. This protocol was used to identify the effect of radiation dose and scan orientation (longitudinal and transversal scans) on the performance of our automatic *CAD–CTC* system.
- Protocol 2: Collimation $1.5\text{ mm} \times 16\text{ mm}$, slice thickness 3 mm, reconstruction interval 1.5 mm, field of view 360 mm, table speed 30 mm/rotation, mAs/rotation: 50, 30, 20 and 13. This protocol was employed to evaluate the influence of the field of view and the variation of the radiation dose.
- Protocol 3: Collimation $1.5\text{ mm} \times 16\text{ mm}$, slice thickness 3 mm, reconstruction interval 1 mm, field of view 325 mm, table speed 30 mm/rotation, mAs/rotation: 100, 80, 70, 60, 50, 40, 30, 20 and 13. This protocol was used to analyse the effect of the reconstruction interval and the radiation dose.
- Protocol 4: Collimation $1.5\text{ mm} \times 16\text{ mm}$, slice thickness 2 mm, reconstruction interval 1 mm, field of view 325 mm, table speed 30 mm/rotation, mAs/rotation: 100, 50, 40, 30, 20 and 13. This protocol was used to generate CT data where the effect of the slice thickness and the radiation dose is analysed.
- Protocol 5: Collimation $1.5\text{ mm} \times 16\text{ mm}$, slice thickness 2 mm, reconstruction interval 0.8 mm, field of view 325 mm, table speed 30 mm/rotation, mAs/rotation: 100, 50, 40, 30, 20 and 13. This protocol was employed to analyse the joint effect of the slice thickness, reconstruction interval and radiation dose.
- Protocol 6: Collimation $1.5\text{ mm} \times 16\text{ mm}$, slice thickness 3 mm, reconstruction interval 1.5 mm, field of view 325 mm, table speed 20 mm/rotation, mAs/rotation: 100, 50, 40, 30 and 20. This protocol was used to find the effect of table speed at different radiation doses.
- Protocol 7: Collimation $0.75\text{ mm} \times 16\text{ mm}$, slice thickness 1 mm, reconstruction interval 0.7 mm, field of view 325 mm, table speed 30 mm/rotation, mAs/rotation: 100, 60, 40, 30 and 22. This protocol was used to find the effect of collimation and radiation doses on the performance of our automatic *CAD–CTC* system.

3. CAD–CTC polyp detection algorithm

We have developed an automated *CAD–CTC* method designed to identify the colorectal polyps in CT data [34] that evaluates the local morphology of the colon wall. Initially, the colon is segmented using a seeded 3D region growing algorithm that was applied to segment the air voxels, which assures the robust identification of the colon wall. In some situations the colon is collapsed due to either insufficient insufflation or residual water. In order to address this issue we have developed a novel colon segmentation algorithm that is able to correctly identify the colon segments using knowledge about their sizes and location within the body in all imaging conditions (for more details refer to [60]). After the identification of the colon wall, the normal vector is calculated for each voxel of the colon wall using the Hummel–Zucker operator [61]. The normal vectors sample the local orientation of the colonic surface and the suspicious candidate structures that may resemble polyps are extracted using a simple convexity analysis. The suspicious colonic surfaces (candidate surfaces) have convex properties and are detected using the 3D histogram and the Gaussian distribution of the Hough Points (for a detailed description of this algorithm refer to [34]). This method is able to correctly identify all polyps above 3 mm but it is worth noting that this is achieved at the cost of a high level of false positives. In order to reduce the level of false positives, statistical features [34] including the standard deviation of surface variation, ellipsoid fitting error, sphere fitting error, three axes of the ellipsoid and the Gaussian sphere radius are calculated for each candidate surface that has been identified by the convexity method described before. These features are fed into a feature normalised classifier [62] that is able to decide whether the surface under investigation belongs to a polyp or a fold. The classifier was trained using a collection of 64 polyps and 354 folds that were selected by a radiologist. The developed *CAD–CTC* algorithm was tested on phantom (standard and low dose CT datasets) and real patient data (mAs/rotation of 100) and shows 100% sensitivity for polyps larger than 5 mm with a rate of 4.05 false positives per dataset.

4. Experiments and results

The aim of this paper is to evaluate the influence of the scanning parameters on the overall polyp detection results in *CAD–CTC* systems. In order to evaluate this, the synthetic phantom detailed in Section 2 has been scanned and a total of 51 CT datasets have been acquired using the seven protocols mentioned in Section 2.2.

When the *CAD–CTC* system has been applied to CT data acquired using the Protocol 1, the results indicate that 100% sensitivity has been achieved for polyps larger than 10 mm in both longitudinal and transversal positions for all radiation levels (100–13 mAs/rotation). For medium size polyps (5–10 mm) the sensitivity was 100% in all cases but 20 and

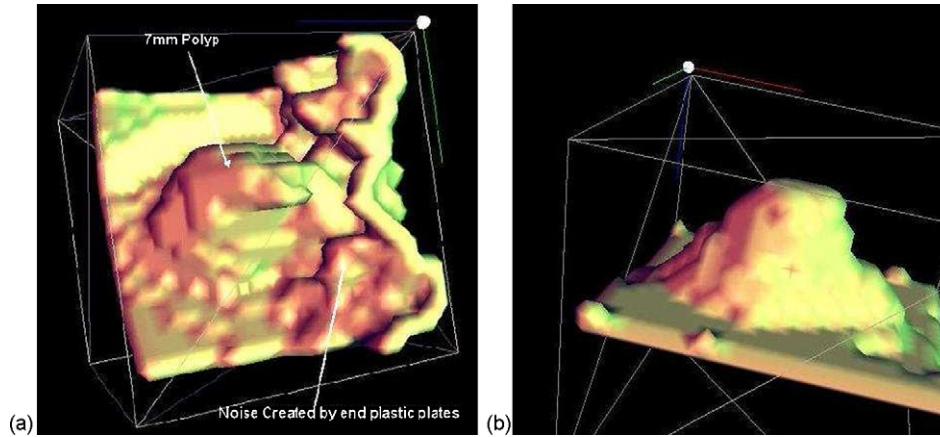


Fig. 4. (a) Polyp undetected by the CAD–CTC algorithm when the data was acquired using the Protocols 1, 3 and 6. (b) Polyp undetected by the CAD–CTC algorithm when the data was acquired using the Protocols 2, 4 and 5.

30 mAs/rotation, where the sensitivity rate was 95%. The reduction in sensitivity was caused by the undetected polyp illustrated in Fig. 4a which was situated close to the end plates. The sensitivity in polyp detection when the CAD–CTC algorithm was applied to CT data acquired using the Protocol 1 is illustrated in Fig. 5.

The sensitivity of the polyp detection achieved when the CAD–CTC algorithm has been applied to CT data acquired using the Protocol 2 is 100% for polyps larger than 10 mm. The sensitivity for medium size polyps (5–10 mm) dropped to 95% when the phantom was scanned with 30, 20 and

13 mAs/rotation. There was only one polyp undetected for data acquired with this protocol and is illustrated in Fig. 4b.

For CT data acquired using the Protocol 3, the polyp detection for all scans show 100% sensitivity except the case when the phantom has been scanned with 30 mAs/rotation. The polyp undetected is illustrated in Fig. 4b. The polyp detection sensitivity when the scans were performed using the Protocol 4 is 100% for polyps larger than 10 mm for all radiation doses except 100 mAs/rotation. The sensitivity in polyp detection for medium size polyps is also 100% except the case when the phantom has been scanned with 30 mAs/rotation when the sensitivity dropped to 95%. The polyp missed by the CAD–CTC system is illustrated in Fig. 4a. The sensitivity in polyp detection obtained when the CAD–CTC system was applied to CT data scanned using the Protocol 5 is lower than the sensitivity obtained when the Protocols 1–4 were employed. The reason for this is that no interpolation was applied to obtain an isometric dataset as the reconstruction interval is 0.8 mm and the voxel resolution is almost the same in all directions (the lower performance of the CAD–CTC system when applied to datasets acquired using the Protocol 5 is justified since the classifier is trained only with interpolated data). Sensitivity achieved for polyp detection when the CAD–CTC algorithm has been applied to CT data obtained using the Protocol 6 is 100% for all radiation doses except the case when the data is scanned with 20 mAs/rotation. The polyp missed by the polyp detection algorithm is illustrated in Fig. 4a. For CT data acquired using the Protocol 7, the polyp detection for all scans shows 100% sensitivity for polyps ≥ 10 mm, (5–10) mm and <5 mm. Results of the automated polyp detection for all 51 scans used in our experiments are depicted in Figs. 5–11. It is useful to note that the overall sensitivity achieved by our CAD–CTC system is lowered by the inclusion of flat polyps. The sensitivity rate for flat polyps is between 22 and 55% and our method has not been designed to detect this class of colorectal polyps. The flat polyps have distinct shapes and their identification should be approached by a CAD–CTC system that is specifically designed to deal with this type of polyps [63].

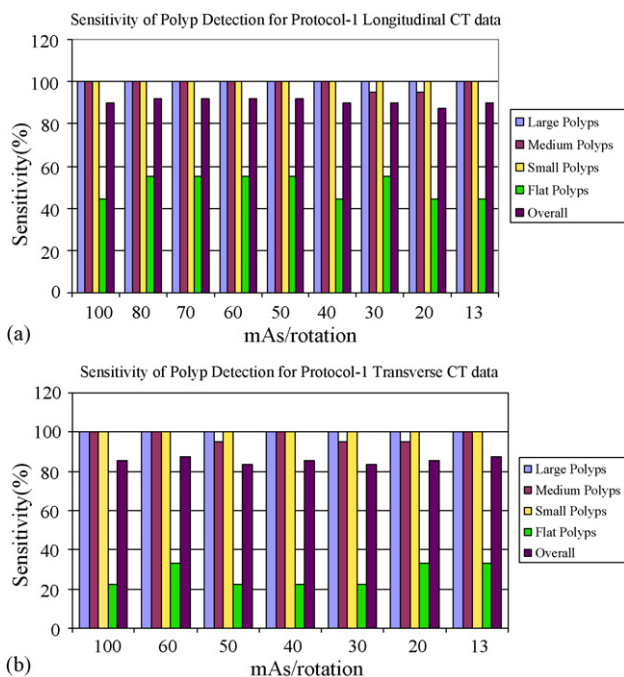


Fig. 5. Sensitivity of the polyp detection algorithm when applied to CT data (Protocol-1: collimation 1.5 mm \times 16 mm, slice thickness 3 mm, reconstruction interval 1.5 mm, field of view 325 mm, table speed 30 mm/rotation) acquired at different radiation doses. (a and b) The sensitivities for Protocol-1 longitudinal and transversal CT data, respectively.

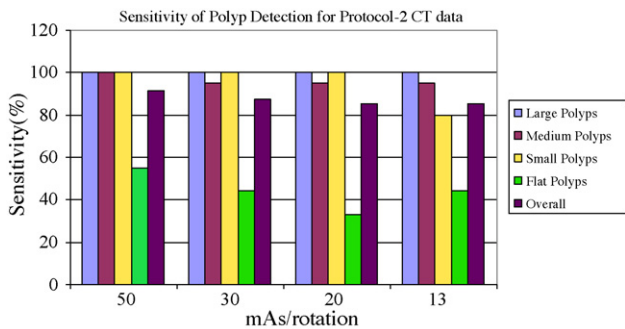


Fig. 6. Sensitivity of the polyp detection algorithm when applied to Protocol-2 CT data.

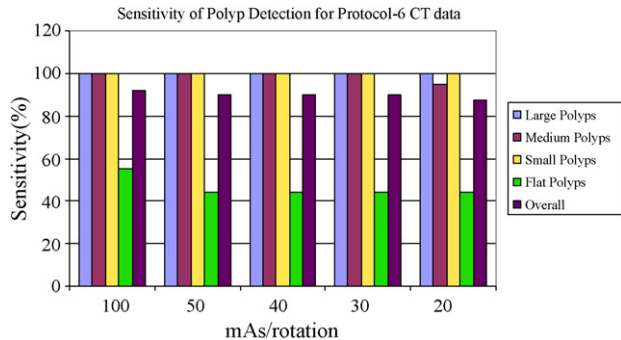


Fig. 10. Sensitivity of the polyp detection algorithm when applied to Protocol-6 CT data.

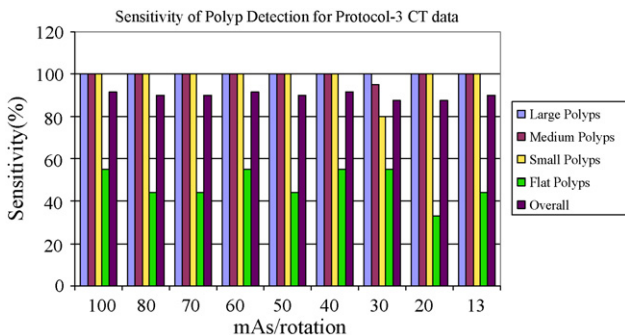


Fig. 7. Sensitivity of the polyp detection algorithm when applied to Protocol-3 CT data.

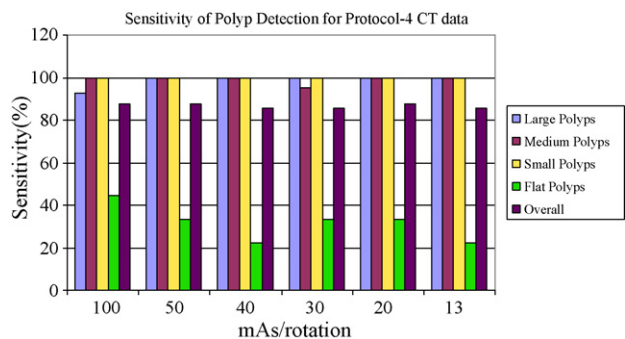


Fig. 8. Sensitivity of the polyp detection algorithm when applied to Protocol-4 CT data.

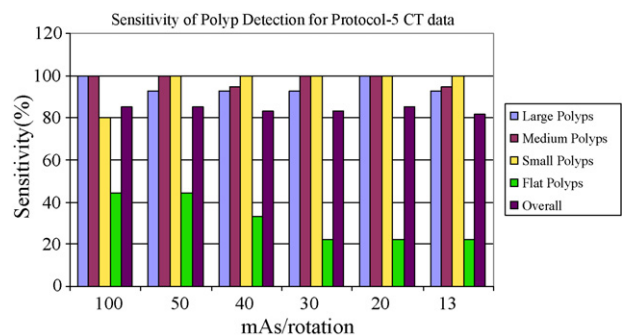


Fig. 9. Sensitivity of the polyp detection algorithm when applied to Protocol-5 CT data.

4.1. Effect of slice thickness, reconstruction interval and table speed

To analyse the effect of slice thickness and reconstruction interval, the synthetic phantom has been scanned using protocols where these parameters are varied (Protocols 1, 3, 4, 5 and 7). An important step preceding the application of the CAD-CTC algorithm is data interpolation. All CT datasets were interpolated in order to make them isometric except cases when they were obtained when the phantom was scanned using the Protocol 5. The CT data obtained using the Protocol 5 was not interpolated as the voxel resolution is almost similar in all directions (voxel width and height: 0.7 mm, voxel depth: 0.8 mm). The experimental results indicate that the performance of the CAD-CTC algorithm is virtually unchanged when it is applied to CT data acquired using the Protocols 1, 3, 4 and 7. The results obtained when the algorithm has been applied to data acquired using the Protocol 5 were worse than those obtained when the algorithm was applied to CT data obtained using other protocols.

This has been generated by the fact that data interpolation has a smoothing effect on the 3D morphology of the colon wall and another important factor is that we have trained the classifier only with interpolated data.

Protocol 7 uses the collimation 0.75 mm × 16 mm that allows us to scan the phantom at a slice thickness of 1mm with a reconstruction interval of 0.7 mm. This protocol was

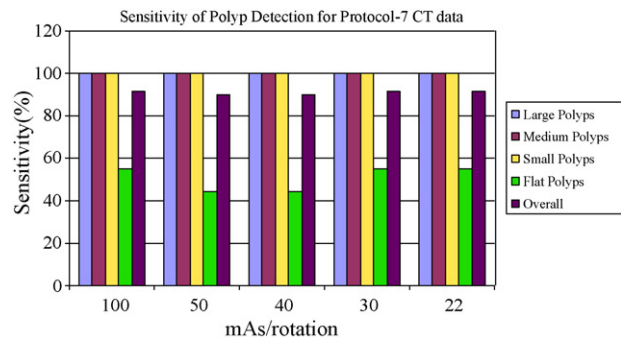


Fig. 11. Sensitivity of the polyp detection algorithm when applied to Protocol-7 CT data.

used to scan the phantom to create near isometric voxels and to evaluate the influence of the lower collimation on the overall performance of the *CAD–CTC* system. Our automatic *CAD–CTC* algorithm shows 100% sensitivity for polyps ≥ 10 mm, (5–10) mm and <5 mm for all doses ranging from 22 to 100 mAs/rotation. As indicated in Fig. 11 our *CAD–CTC* system shows higher sensitivity when applied to 30 mAs/rotation CT data acquired using the Protocol 7 (100%) than in cases when the phantom was scanned at the same radiation dose using the Protocols 1–5. It is useful to note that the small increase in sensitivity noticed when the phantom was scanned using the Protocol 7 is obtained at the expense of a higher rate of false positives (generated by the uneven surface of the phantom) and higher radiation dose.

The field of view was set to 360 mm for Protocol 2 and to 325 mm for other protocols. The experimental data indicates that the field of view does not have a significant impact on the performance of the automated polyp detection algorithm.

Another parameter of interest is the table speed. To evaluate the influence of this parameter on the overall polyp detection results, we set this parameter to 20 mm/rotation for Protocol 6 and 30 mm/rotation for Protocols 1–5 and 7. At 30 and 20 mm/rotation table speeds the effective dose is 2.7 mSv at 100 mAs/rotation for Protocols 1–6. This parameter has a negligible effect on the radiation dose since the Siemens scanner used in our experiments utilises the “effective tube current” model where a variation in the scan time (the lower the scan time the higher the table speed) implies a concomitant variation in the tube current. For Siemens Somatom 16 slice CT scanner the lowest mAs/rotation that can be set at 20 mm/rotation table speed is 20 mAs/rotation whereas for 30 mm/rotation table speed the lowest mAs/rotation is 13. We have varied this parameter to evaluate only the effect of the motion artefacts and the experimental results indicate that the table speed has a marginal effect on the overall performance of our *CAD–CTC* system. Small benefits have been observed when the algorithm has been applied to the detection of small (not clinically significant) and flat polyps.

4.2. Level of noise and the radiation dose

In this element of the study we aim to evaluate the correlation between the image noise and the radiation dose. In this regard we have selected five circular regions of interest (ROIs) with a radius of 20 voxels that are evaluated for three consecutive slices (see Fig. 12). Since the data is homogeneous (the phantom is filled with water) the level of noise can be accurately sampled by calculating the standard deviation (S.D.) of the voxel distribution within the circular region of interest.

For CT data scanned using the Protocols 1 and 3, the S.D. increased with a factor of 2.67 (S.D. = 26.59 for 100 mAs/rotation and S.D. = 70.95 for 13 mAs/rotation) when the scan was performed at 13 mAs/rotation when compared to the case when the phantom was scanned with 100 mAs/rotation radiation dose. The relation between the

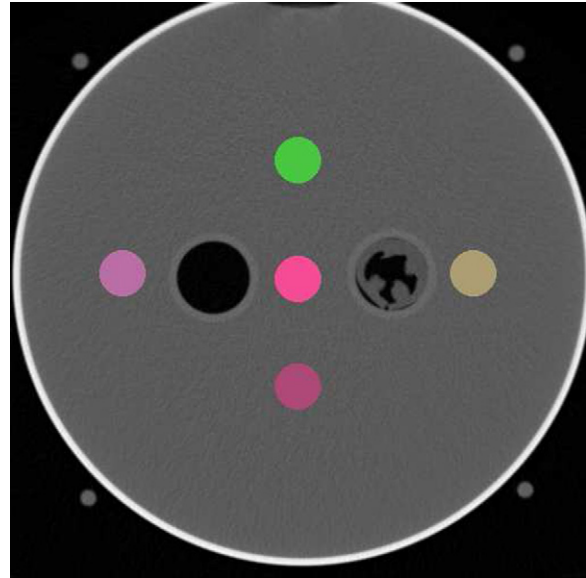


Fig. 12. Five regions of interests located on the phantom to evaluate the noise level.

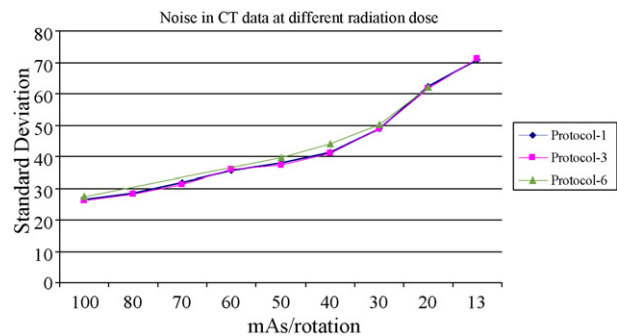


Fig. 13. The relationship between noise level and the radiation dose.

noise level and the radiation dose is almost linear and this is illustrated in Fig. 13. In Fig. 13 is noticed a small decay in the plot for Protocol 1 that may be caused by the smoothing effect induced by the data interpolation procedure.

5. Conclusions

The experimental data presented in this paper is obtained by scanning the synthetic phantom described in Section 2.1. Although the phantom was designed to emulate as closely as possible the real clinical conditions it is worth noting that the synthetic data is not affected by factors such as motion artefacts (caused by breathing) or the presence of residual material such as fluid and stool that are currently experienced when analysing real patient data. One of the main aims of this investigation was the development of a study environment that allows us to determine the influence of the scanning parameters on the performance of the polyp detection algorithm. Currently, the performance of the existing *CAD–CTC* systems is evaluated on real patient data that is supplied by differ-

ent research organizations that are not available for computer vision community. Therefore the absence of standard test data makes the performance evaluation of these systems restricted to the scenario they were tested. Thus, another important merit of this investigation is the generation of ground truth synthetic data that can be used to test all developed systems in the same conditions. For comparison purposes we have made the phantom data available on request from the following web page: <http://www.eeng.dcu.ie/~whelanp/cadctc>. Typical size of a CT dataset is in the range (70–125 MB). It is useful to note that recently the Walter Reed Army Medical Center (WRAMC) database has been made available to the research community which will help the evaluation of the developed *CAD–CTC* systems but the main advantage of using synthetic data is the generation of unambiguous ground truth data (requires no validation by radiologists) that can be used especially in the development phase of the *CAD–CTC* systems.

Our *CAD–CTC* system indicates that automated polyp detection is feasible even at radiation doses as low as 13 mAs/rotation. The sensitivity rate in polyp detection achieved by our *CAD–CTC* system is always higher than 90% for polyps larger than 5 mm and the overall sensitivity for all types of polyps is higher than 80%. The sensitivity rate would be even higher as our method has not been trained for the detection of flat polyps. For this type of polyps the achieved sensitivity is in the range 22–55%. In our experiments one polyp (see Fig. 4a) has been placed closed to the outer plastic plates of the phantom and at low radiation doses the image noise joined the surface of the polyp with the surface generated by the plastic plate and the classifier assigned this surface to be part of a fold. It is worth mentioning that this situation will not appear in clinical studies.

The main merit of this paper is the development of a realistic phantom that closely simulates the situations encountered in real clinical studies. Thus, we placed the main emphasis on evaluating the influence of the scanning parameters on the performance of the automated polyp detection. From these parameters we focused our attention on the radiation dose as the main concern regarding CT examinations is the exposure of the patients to ionizing radiation. Recent studies demonstrated that CT which accounts for 4% of the medical radiographic examinations contributes 35–40% of the cumulated radiation dose received by the patients [64]. Our study reveals that the reduction of mAs/rotation from 100 to 13 (1.5 mm × 16 mm collimation) reduced the effective dose from 2.7 to 0.35 mSv as it is illustrated in Fig. 14. In our experiments we have also scanned the phantom using a reduced collimation (0.75 mm × 16 mm) but the experimental data indicates that the small increase in polyp detection sensitivity achieved by our *CAD–CTC* system does not justify the increased radiation dose that would be received by patients (there will be an 11% increase of the effective dose as illustrated in Fig. 14). In addition it is worth noting that the volume of CT data acquired at a reduced collimation is significantly larger than the volume of CT data generated

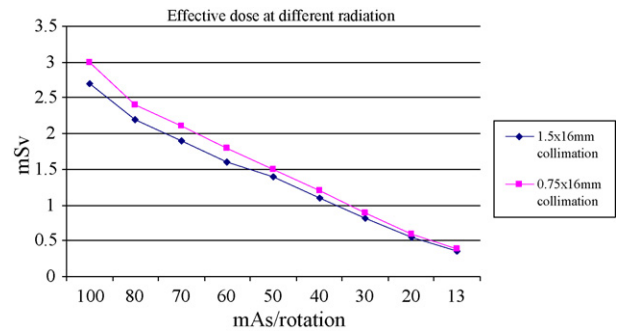


Fig. 14. Radiation dose received by the patient at different mAs/rotation using the ImPACT dosimetry tool [65].

at 1.5 mm × 16 mm collimation and this will be a deterring factor when the data is evaluated manually by radiologists. We conclude that a reduced collimation is not justified since the increase in sensitivity is marginal and for clinical purposes a 1.5 mm × 16 mm collimation is deemed appropriate to detect the clinically significant colorectal polyps (see the results reported in Figs. 5–10 (1.5 mm × 16 mm collimation) and Fig. 11 (0.75 mm × 16 mm collimation)).

Also another important issue we tried to address in this paper is the relationship between the radiation dose and the impact on the performance of the *CAD–CTC* polyp detection algorithm. In this regard, our studies indicated that the level of image noise when the phantom was scanned with 13 mAs/rotation was higher with a factor of 2.67 than in the case when the phantom was scanned with 100 mAs/rotation radiation dose. Although the level of noise significantly increased at low radiation dose the effect on the performance in polyp detection is minimal. The experimental data presented in Figs. 5–11 indicates that the sensitivity in polyp detection for polyps larger than 5 mm is always above 95%. We notice a small increase in false positives at 13 mAs/rotation but the effect on true positive detection rate is not noticeable. The impact of the field of view and the reconstruction interval was negligible and it was virtually eliminated by the smoothing effect of the data interpolation that is applied to make the dataset isometric. We conclude that low dose radiation (as low as 13 mAs/rotation) is feasible to be used in standard CTC clinical examinations.

Acknowledgements

We would like to acknowledge the contributions of our clinical partners in this project: Dr. Helen Fenlon (Department of Radiology) and Dr. Padraic Mac-Mathuna (Gastrointestinal Unit) of the Mater Misericordiae Hospital, Dublin. We would also like to acknowledge our colleague Robert Sadleir for the development of the DICOM decoder software. This work was supported under an Investigator Programme Grant (02/IN1/1056) by Science Foundation Ireland (SFI). Finally, we would like to thank the anonymous reviewers for their helpful feedback.

References

- [1] Parker S, Tong T, Bolden S, Wingo P. Cancer statistics 1997. *CA Cancer J Clin* 1997;47:5–27.
- [2] NCRI, 2000. Cancer in Ireland, incidence and mortality. Healy & Associates; 1997.
- [3] Cancer Research UK, Bowel cancer factsheet, 2003.
- [4] Ransoh DF, Sandler RS. Screening for colorectal cancer. *New Engl J Med* 2002;346(1).
- [5] American Cancer Society. Cancer facts and figures. American Cancer Society; 1999.
- [6] National Cancer Institute. Working guidelines for early cancer detection: rationale and supporting evidence to decrease mortality. Bethesda: National Cancer Institute; 1987.
- [7] Robert A, Cokkinides SV, Eyre HJ. American Cancer Society guidelines on the early detection of cancer. *Cancer J Clin* 2003;53:27–43.
- [8] Schrock TR. Colonoscopy versus barium enema in the diagnosis of colorectal cancer and polyps. *Gastrointest Endosc Clin N Am* 1993;3:585–610.
- [9] Winawer JS, Stewart ET, Zauber AG, Bond JH. A comparison of colonoscopy and double-contrast barium enema for surveillance after polypectomy. *New Engl J Med* 2000;342:1766–72.
- [10] Sato M, Lakare S, Wan M, Kaufman A, Liang Z, Wax M. An automatic colon segmentation for 3D virtual colonoscopy. *IEICE Trans Inform Syst* 2001;E84-D(1):201–8.
- [11] Vining DJ, Gelfand DW, Bechtold RE, Scharling ES, Grishaw EK, Shifrin RY. Technical feasibility of colon imaging with helical CT and virtual reality. *Am J Roentgenol* 1994;162:104.
- [12] Johnson CD, Hara AK, Reed JE. Virtual endoscopy: what's in a name? *Am J Roentgenol* 1998;171:1201–2.
- [13] Lichan H, Arie K, Chih WYi, Ajay V, Mark W, Zhengrong L. 3D virtual colonoscopy. In: Loew M, Gershon N, editors. Proceedings of the biomedical visualization. 1995. p. 26–33.
- [14] Hara AK, Johnson CD, Reed JE, Ahlquist DA, Nelson H, Ehman RL. Detection of colorectal polyps by CT colonography: feasibility of a novel technique. *Gastroenterology* 1996;100:284–90.
- [15] Hong L, Muraki S, Kaufman A, Bartz D, He T. Virtual voyage: interactive navigation in the human colon. In: Proceedings of the ACM SIGGRAPH. 1997. p. 27–34.
- [16] Wan M, Tang Q, Kaufman A, Liang Z, Wax M. Volume rendering based interactive navigation within the human colon. In: Proceeding of the IEEE visualization. 1999. p. 397–400.
- [17] Sezille N, Sadleir RJT, Whelan PF. Fast extraction of planes normal to the centreline from CT colonography datasets. In: VIE 2003—IEE visual information engineering conference. 2003.
- [18] Sadleir RJT, Whelan PF. Fast colon centreline calculation using optimised 3D topological thinning. *Comput Med Imag Graph* 2005;29(4):251–8.
- [19] Bartroli AV, Wegenkittl R, Konig A, Groller E. Nonlinear virtual colon unfolding. In: Proceedings of the twelfth IEEE visualization (VIS'01). 2001.
- [20] Vining DJ, Hunt GW, Ahn DK, Stelts DR, Helmer PF. Computer assisted detection of colon polyps and masses. *Radiology* 2001;219:51–9.
- [21] Summers RM, Johnson CD, Pusanik LM, Malley JD, Youssef AM, Reed JE. Automated polyp detection at CT colonography: feasibility assessment in a human population. *Radiology* 2001;219:51–9.
- [22] Summers RM, Beaulieu CF, Pusanik LM, Malley JD, Jeffrey RB, Glazer DI, et al. Automated polyp detector for CT colonography: feasibility study. *Radiology* 2000;216:284–90.
- [23] Yoshida H, Masutani Y, MacEneaney P, Rubin DT, Dachman AH. Computerized detection of colonic polyps at CT colonography on the basis of volumetric features: pilot study. *Radiology* 2002;222:327–36.
- [24] Yoshida H, Nappi J. Three-dimensional computer-aided diagnosis scheme for detection of colonic polyps. *IEEE Trans Med Imag* 2001;20(12):1261–74.
- [25] Paik DS, Beaulieu CF, Rey RBJ. Computer aided detection of polyps in CT colonography: method and free-response ROC evaluation of performance. *Radiology* 2000;217 (P):370.
- [26] Kiss G, Cleynenbreugel J, Thomeer M, Suetens P, Marchal G. Computer aided diagnosis for virtual colonography. *Med Image Comput Comput-Assist Intervent* 2001:621–8.
- [27] Kiss G, Cleynenbreugel J, Thomeer M, Suetens P, Marchal G. Computer aided detection of colonic polyps via geometric feature classification. *Vision Model Visual* 2002:27–34.
- [28] Kiss G, Cleynenbreugel J, Suetens P, Marchal G. Computer aided diagnosis for CT colonography via slope density functions. *Med Image Comput Comput-Assist Intervent* 2003:746–53.
- [29] Paik DS, Beaulieu CF, Rubin GD, Acar B, Jeffrey Jr RB, Yee J, et al. Surface normal overlap: a computer-aided detection algorithm with application to colonic polyps and lung nodules in helical CT. *IEEE Trans Med Imag* 2004;23(6):661–75.
- [30] Kiraly AP, Laks S, Macari M, Geiger B, Bogoni L, Novak CL. A fast method for colon polyp detection in high-resolution CT data. *Int Congr Ser* 2004;1268:983–8.
- [31] Acar B, Napel S, Paik D, Gokturk SB, Tomasi C, Beaulieu CF. Using optical flow fields for polyp detection in virtual colonoscopy. Utrecht, Holland: Medical Image Computing and Computer-Assisted Intervention; 2001.
- [32] Wang Z, Li L, Anderson J, Harrington D, Liang Z. Colonic polyp characterization and detection based on both morphological and texture features. *Int Congr Ser* 2004;1268:1004–9.
- [33] Jerebko AK, Malley JD, Franaszek M, Summers RM. Multi neural network classification scheme for detection of colonic polyps in CT colonography data sets. *Acad Radiol* 2003;10(2):154–60.
- [34] Chowdhury TA, Ghita O, Whelan PF. A statistical approach for robust polyp detection in CT colonography. In: Proceedings of the twenty-seventh annual international conference of the IEEE Engineering in Medicine and Biology Society, September 1–4. 2005.
- [35] Barnes E. Colon CAD: VC's extra eyes face new challenges, <http://auntminnie.com/>, August 5, 2005.
- [36] Yee J, Akerkar GA, Hung RK, Steinauer-Gebauer AM, Wall SD, McQuaid KR. Colorectal neoplasia: performance characteristics of CT colonography for detection in 300 patients. *Radiology* 2001;219:685.
- [37] Fletcher JG, Johnson CD, Krueger WR, Ahlquist DA, Nelson H, Ilstrup D, et al. Contrast-enhanced CT colonography in recurrent colorectal carcinoma: feasibility of simultaneous evaluation for metastatic disease, local recurrence, and metachronous neoplasia in colorectal carcinoma. *Am J Roentgenol* 2002;178(283–290).
- [38] Hoon J, Rolnick JA, Haker S, Barish MA. Multislice CT colonography: current status and limitations. *Eur J Radiol* 2003;47(2):123–34.
- [39] Sosna J, Morrin MM, Kruskal JB, Farrell RJ, Nasser I, Raptopoulos V. Colorectal neoplasms: role of intravenous contrast-enhanced CT colonography. *Radiology* 2003;228(1):152–6.
- [40] Filippone A, Ambrosini R, Fuschi M, Marinelli T, Genovesi D, Bonomo L, et al. N staging of colorectal cancer: accuracy of contrast-enhanced multi-detector row CT colonography—initial experience. *Radiology* 2004;231(1):83–90.
- [41] Gelder REV, Venema HW, Florie J, Yung C, Serlie IWO, Schutter MP, et al. CT colonography: feasibility of substantial dose reduction—comparison of medium to very low doses in identical patients. *Radiology* 2004;232:611–20.
- [42] Brenner DJ, Elliston CD, Hall EJ. Estimated risks of radiation induced fatal cancer from pediatric CT. *Am J Roentgenol* 2001;176:289–96.
- [43] Cohen BL. Cancer risk from low-level radiation. *Am J Roentgenol* 2002;179:1137–43.
- [44] Iannaccone R, Laghi A, Catalano C, Brink JA, Mangiapane F, Trenna S, et al. Detection of colorectal lesions: lower-dose multi-detector row helical CT colonography compared with conventional colonoscopy. *Radiology* 2003;229:775–81.
- [45] Capunay CM, Carrascosa PM, Bou-Khair A, Castagnino N, Ninomiya I, Carrascosa JM. Low radiation dose multislice CT colonog-

- raphy in children: Experience after 100 studies. *Eur J Radiol* 2005;56(3):398–402.
- [46] Vogt C, Cohnen M, Beck A, Dahl SV, Aurich V, Modder U, et al. Detection of colorectal polyps by multislice CT colonography with ultra-low-dose technique: comparison with high-resolution videocolonoscopy. *Gastrointest Endosc* 2004;60(2):201–9.
- [47] Beaulieu CF, Napel S, Daniel BL, Ch'en IY, Rubin GD, Johnstone IM, et al. Detection of colonic polyps in a phantom model: implications for virtual colonoscopy data acquisition. *J Comput Assist Tomogr* 1998;22(4):656–63.
- [48] Dachman AH, Lieberman J, Osnis RB, Chen SY, Hoffmann KR, Chen CT, et al. Small simulated polyps in pig colon: sensitivity of CT virtual colonography. *Radiology* 1997;203:427–30.
- [49] Taylor SA, Halligan S, Bartram CI, Morgan PR, Talbot IC, Fry N, et al. Multi-detector row CT colonography: effect of collimation, pitch, and orientation on polyp detection in human colectomy specimen. *Radiology* 2003;229:109–18.
- [50] Springer P, Stohr B, Giacomuzzi SM, Bodner G, Klingler A, Jaschke W, et al. Virtual computed tomography colonoscopy: artifacts, image quality and radiation dose load in a cadaver study. *Eur Radiol* 2000;10(1):183–7.
- [51] Whiting BR, McFarland EG, Brink JA. Influence of image acquisition parameters on CT artifacts and polyp detection in spiral CT colonography: in vitro evaluation. *Radiology* 2002;217:165–72.
- [52] Power NP, Pryor MD, Martin A, Horrocks J, McLean AM, Reznick RH. Optimization of scanning parameters for CT colonography. *Br J Radiol* 2002;75:401–8.
- [53] Wessling J, Fischbach R, Meier N, Allkemper T, Klusmeier J, Ludwig K, et al. CT colonography: protocol optimization with multi-detector row CT-study in an anthropomorphic colon phantom. *Radiology* 2003;228:753–9.
- [54] Laghi A, Iannaccone R, Mangiapane F, Piacentini F, Iori S, Passariello R. Experimental colonic phantom for the evaluation of the optimal scanning technique for CT colonography using a multi-detector spiral CT equipment. *Eur Radiol* 2003;13(3):459–66.
- [55] Embleton KV, Nicholson DA, Hufton AP, Jackson A. Optimization of scanning parameters for multi-slice CT colonography: experiments with synthetic and animal phantoms. *Clin Radiol* 2003;58(12):955–63.
- [56] Ozgun A, Rollven E, Blomqvist L, Bremmer S, Odh R, Fransson A. Polyp detection with MDCT: a phantom-based evaluation of the impact of dose and spiral resolution. *Am J Roentol* 2005:184.
- [57] Ling SH, Summers RM, Loew MH, McCollough CH, Johnson CD. Computer-aided detection of polyps in a colon phantom: effects of scan orientation, polyps size, collimation and dose. *J Comput Assist Tomogr* 2002;26(6):1013–8.
- [58] Sundaram P, Beaulieu CF, Paik DS, Schraedley-Desmond P, Napel S. CT colonography: does improved z resolution help computer-aided polyp detection? *Med Phys* 2003;30(10):2663–74.
- [59] NHS Purchasing and Supply Agency, Report 05071, Siemens Somatom Sensation open CT scanner technical evaluation, December 2005.
- [60] Chowdhury TA, Whelan PF, Ghita Ovidiu. A method for automatic segmentation of collapsed colons at CT colonography. In: Proceedings of the second Indian international conference on artificial intelligence. 2005.
- [61] Zucker SW, Hummel RA. A three-dimensional edge operator. *IEEE Trans Pattern Anal Mach Intell* 1981;3(3):324–31.
- [62] Ghita O, Whelan PF. A bin picking system based on depth from focus. *Mach Vis Appl* 2003;13:234–44.
- [63] Park SH, Ha HK, Kim AY, Kim KW, Lee MG, Kim PN, et al. Flat polyps of the colon: detection with 16-MDCT colonography preliminary results. *Am J Roentol* 2006;186:1611–7.
- [64] Nagel HD. Radiation exposure in computed tomography. Frankfurt, Germany: European Coordinate Committee of the Radiological and Electromedical Industries, COCIR; 2000.
- [65] ImPACT CT patient dosimetry calculator, <http://www.impactscan.org/ctdosimetry.htm>.